LETTERS

Simulation of equatorial and high-latitude jets on Jupiter in a deep convection model

Moritz Heimpel[1], Jonathan Aurnou[2] & Johannes Wicht[3]

The bands of Jupiter represent a global system of powerful winds. Broad eastward equatorial jets are flanked by smaller-scale, higher-latitude jets flowing in alternating directions[1,2]. Jupiter's large thermal emission suggests that the winds are powered from within[3,4], but the zonal flow depth is limited by increasing density and electrical conductivity in the molecular hydrogen–helium atmosphere towards the centre of the planet[5]. Two types of planetary flow models have been explored: shallow-layer models reproduce multiple high-latitude jets, but not the equatorial flow system[6–8], and deep convection models only reproduce an eastward equatorial jet with two flanking neighbours[9–14]. Here we present a numerical model of three-dimensional rotating convection in a relatively thin spherical shell that generates both types of jets. The simulated flow is turbulent and quasi-two-dimensional and, as observed for the jovian jets, simulated jet widths follow Rhines' scaling theory[2,12,13,15]. Our findings imply that Jupiter's latitudinal transition in jet width corresponds to a separation between the bottom-bounded flow structures in higher latitudes and the deep equatorial flows.

Turbulent energy typically passes from larger to smaller scales. However, this process can reverse under conditions favouring coherent flow. This is the case for rapid planetary rotation (geostrophy), where small-scale turbulent motions can feed large-scale zonal jets—a process that seems to be discernible from analysis of the jovian surface winds[15]. The effects of boundary curvature in a rotating system are quantified by a parameter β. The inverse cascade from small to large scales ceases at the Rhines length, which is inversely proportional to β and sets the characteristic width of zonal jets[16]. For a shallow planetary layer, with fluid motion constrained to the outer spherical surface, β depends upon the latitudinal variation of the local strength of planetary rotation[12,13,16]. On the other hand, turbulent flow in a rapidly rotating spherical volume generates deep cylindrically symmetric flow structures aligned with the rotation axis. Deep zonal flow is governed by the topographic β-parameter, which depends on the gradient of the axial fluid column height, and has sign opposite to that of β for a shallow layer. This sign difference implies that a shallow layer produces retrograde (westward) equatorial flow as observed on Uranus and Neptune, whereas full-sphere dynamics results in a prograde (eastward) equatorial jet, as on Jupiter and Saturn[6,12].

The existence of an inner spherical boundary modifies deep zonal flow by separating it into three connected but dynamically distinct regions (north, equatorial and south), bounded by the tangent cylinder that circumscribes the inner boundary equator. The radius ratio $\chi = r_i/r_o$ sets the location of the tangent cylinder and is of fundamental importance to rapidly rotating convection. Figure 1 illustrates the structure of geostrophic zonal flow in a spherical shell. Inside the tangent cylinder, northern and southern flow structures are separated by the inner boundary. In contrast, flow structures extend over both hemispheres in the equatorial region. The tangent cylinder therefore corresponds to a scaling discontinuity. Starting at the equator, the axial column height increases with latitude. Outside the tangent cylinder, scaling is identical to that of a full sphere, and the sign of β is consistent with a prograde equatorial jet. Crossing the latitude θ_{tc}, where the tangent cylinder intersects the outer surface, the column height is reduced by one-half, β changes sign, and fluid columns decrease in height toward the pole[17]. Because of this sign reversal, jet scaling inside the tangent cylinder is analogous to that of a shallow layer. (Indeed, the limiting case of a very thin three-dimensional spherical shell is equivalent to a two-dimensional layer.) Furthermore the jump in β decreases the Rhines length inside the tangent cylinder, favouring the formation of multiple jets there.

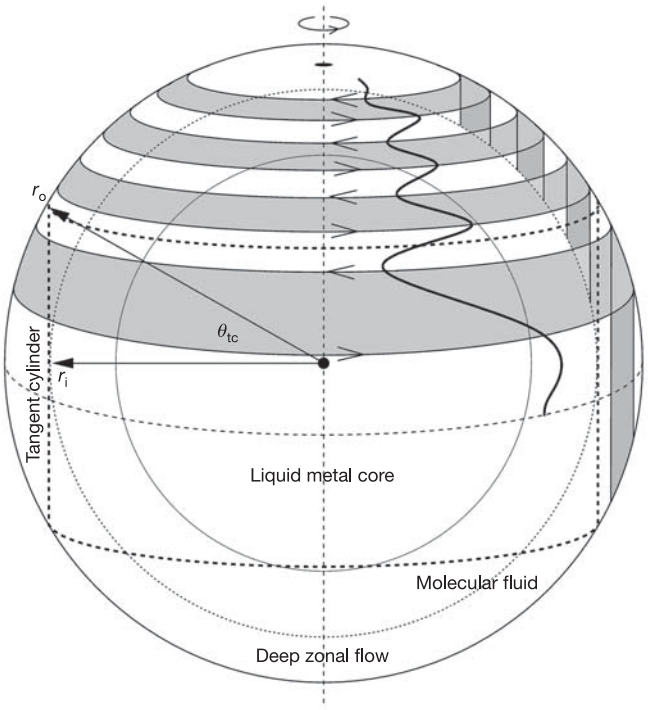

Figure 1 | Illustration of rapidly rotating turbulent convection in a spherical shell. Flow occurs between outer radius r_o and inner radius r_i. The latitudes $\theta_{tc} = \pm\cos^{-1}(r_i/r_o)$ mark the intersection of the tangent cylinder with the outer boundary. The shaded and white areas in the northern hemisphere correspond (on the outer surface) to the visible jovian belts and zones[1]. The radius ratio shown here, and the size of the liquid metal core, are chosen for the purpose of illustration and do not represent estimates for Jupiter. The origin of Jupiter's visible colours is not addressed in this paper.

[1]Department of Physics, University of Alberta, Edmonton, Alberta, T6G 2J1, Canada. [2]Department of Earth and Space Sciences, UCLA, Los Angeles, California 90095-1567, USA. [3]Max Planck Institute for Solar System Research, 37191 Katlenburg-Lindau, Germany.

Previous analytical models of planetary zonal flow in a spherical shell have assumed a relatively deep bottom boundary, such that high-latitude zonal jets develop from flows outside the tangent cylinder[18]. More recent numerical models of deep and strongly turbulent three-dimensional quasigeostrophic convection[10,11] have produced jets of realistic amplitudes. However, these moderately thick fluid shells (with radius ratios $\chi = r_i/r_o = 0.6$–0.75) produce only a pair of high-latitude jets in each hemisphere inside the tangent cylinder[10,14], which cannot account for the observed pattern of jovian jets. Laboratory experiments of rotating convection in deep spherical shells[19] with $\chi = 0.35$ and 0.70 have obtained zonal flow patterns that are broadly comparable to the results of spherical numerical models[9,10]. However, multiple jets have been produced by idealized numerical[20] and experimental[21] models with a cylindrical geometry, a free top surface, and a sloping bottom surface. In those local models, as well as our present global model, the jets are produced by the topographic β-effect and follow Rhines scaling.

There are various possible reasons why previous spherical shell models have not produced multiple higher-latitude jets. Instead of analysing particular cases we list the following conditions that favour the development of multiple high-latitude jets. Turbulent flow (that is, high Reynolds number) constrained by rapid rotation (that is, low Rossby number) is necessary for the development of jets that follow Rhines scaling. A relatively thin fluid layer allows multiple jets to form at higher latitudes by decreasing the Rhines length and increasing the latitudinal range inside the tangent cylinder.

We use numerical modelling to study turbulent thermal convection in a rapidly rotating three-dimensional spherical shell, with simulation parameters chosen to reflect our present understanding of Jupiter's interior. The spherical shell geometry is defined by the radius ratio $\chi = r_i/r_o$. We have chosen $\chi = 0.9$, which represents a substantially thinner shell than in previous models of rotating convection[10,14]. This value of the radius ratio corresponds to a depth in Jupiter of approximately 7,000 km, which is shallower than the phase boundary that separates the outer molecular fluid from the liquid metal H–He core, estimated at 0.8–0.85 R_J, where $R_J \approx 70{,}000$ km is the radius of Jupiter[13]. Measurements of increasing flow velocity with depth suggest that the surface winds are seated in the deep molecular H_2–He atmosphere[22]. However, increasing density and electrical conductivity with pressure result in inertial and Lorentz forces that are expected to damp the zonal flow between 0.85 and 0.95 R_J (refs 13 and 23). Thus we have chosen a simulation radius ratio that lies near the middle of current estimates. A description of Saturn's interior is similar to that of Jupiter except that lower saturnian gravity roughly doubles the estimated layer depth.

Selection of other simulation parameters (see Methods) is based on recent numerical and experimental scaling analyses for convection-driven zonal flows in thicker spherical shells[11,24]. An essential ingredient in this numerical simulation is that convective turbulence is quasigeostrophic and close to the asymptotic state of rapid rotation in which viscosity and thermal diffusivity play a negligible role in the dynamics. Thus, large discrepancies between the simulation parameters and those estimated for Jupiter should not strongly affect the character of the solution. We do not model the jovian troposphere, nor the effects of latitudinally varying insolation[7,8]. Furthermore, we model convection only within the region where large-scale zonal flows are predicted to occur and we neglect deeper regions where convection may be vigorous but zonal flows are expected to be weak. Although fluid compressibility effects are important to the dynamics of convection in the gas giants[25], the fluid in our numerical model is assumed to be incompressible except for thermal buoyancy effects (that is, the Boussinesq approximation). The omission of compressibility effects is possibly this model's greatest limitation. However, considering that we use a relatively thin convection layer, a Boussinesq treatment may be adequate to simulate the large-scale dynamics[12,13].

Figure 2 shows the results of our numerical simulation and the jovian zonal wind pattern. Figure 2a is a plot of Jupiter's averaged surface azimuthal (east–west) velocity profile relative to the deep-seated magnetic-field reference frame[1]. Although we focus here on

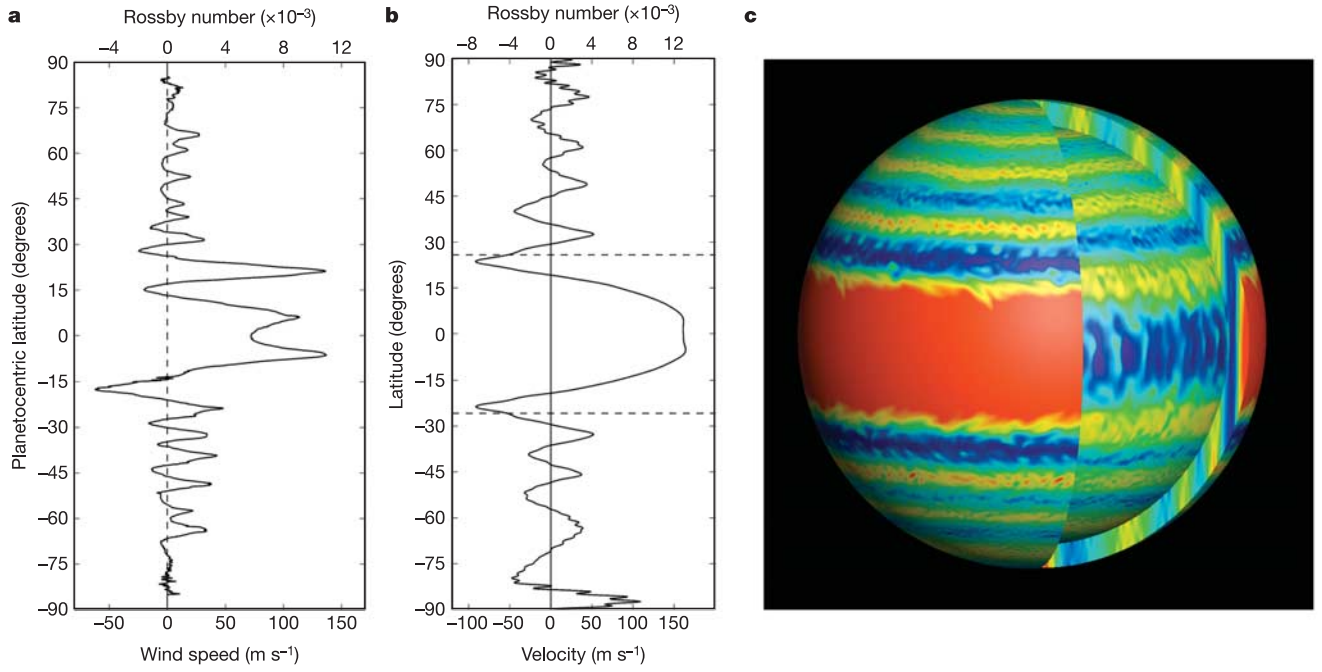

Figure 2 | Zonal flow for Jupiter and the numerical simulation. **a**, The zonal wind of Jupiter. The Cassini space mission data was kindly provided by A. Vasavada. Wind speed may be converted to Rossby number using $\mathrm{Ro} = \nu/\Omega r_o$). **b**, Snapshot in time of the simulation's outer-surface azimuthally averaged azimuthal (east–west) velocity. Dashed lines indicate the latitude where the tangent cylinder intersects the outer surface, for the simulation's radius ratio ($\chi = r_i/r_o = 0.9$). **c**, Snapshot of the simulation's azimuthal velocity field on the outer and inner spherical surface, and on a meridional slice. Red and blue colours represent prograde (eastward) and retrograde (westward) flow, respectively.

Jupiter, it is noted that Saturn has a comparable wind pattern, with a stronger and broader eastward equatorial jet and roughly half the number of high-latitude jets. Figure 2b and c shows aspects of the flow field resulting from the numerical model. In the simulation, a prominent equatorial jet is underlaid by flow structures that are aligned with the rotation axis and span the two hemispheres. At higher latitudes, multiple alternating jets form a series of banded flows that are underlaid by axially aligned flow structures bounded by the outer and inner spherical surfaces. The cylindrical symmetry of the simulation's global flow field shows that it is quasigeostrophic.

To test the applicability of the spherical shell model to Jupiter we compare the simulated and jovian jet scaling to that predicted by the theory of geostrophic turbulence. Analysis of Rhines scaling in spherical shell geometry (see Methods) results in predicted jet widths based on the mean zonal flow velocity within the three regions bounded by the tangent cylinder (north, equatorial and south). Predicted versus measured jet widths are plotted in Fig. 3. For both Jupiter and our numerical model, the jet widths are relatively narrow and constant at high latitudes and increase sharply toward the equator. The simulated equatorial jets are broader than predicted, which suggests that, in our simulation, Rhines scaling is not dominant outside the tangent cylinder. However, at higher latitudes the simulated jet widths clearly follow Rhines scaling, and the equatorward increase in jet widths occurs, as expected, at the latitude of the tangent cylinder. A similar scaling transition is also evident for the jovian jet widths. This scaling transition is predicted for turbulent convection in a rapidly rotating spherical shell, but not for a full sphere or a two-dimensional shallow layer.

Current understanding of Jupiter's zonal winds is based largely upon observations of the surface motions and heat flow. Additional constraints on the nature and extent of deep flows could come from accurate measurements of the planetary gravitational field. Deep zonal flows can carry significant angular momentum, enough to generate measurable latitudinal gravity variations[26]. Further evidence could involve higher-resolution observations of Jupiter's outward heat flux. Such evidence will be provided by future space missions, including the planned jovian polar orbiter Juno[27].

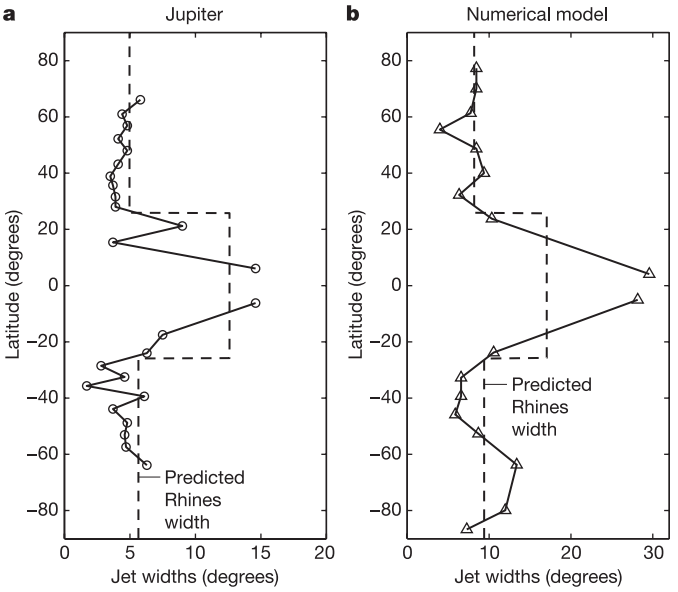

Figure 3 | Measured jet widths compared to jet widths predicted by Rhines scaling for Jupiter (a) and the numerical model (b). Circle and triangle symbols represent individual jet measurements (see Supplementary Information for jet-measurement method). Predicted widths (dashed black lines) are obtained from observed regional (north, equatorial, and south) zonal velocities (see equation (3) in the Methods section). The latitude of the discontinuity in predicted jet widths represents the intersection of the tangent cylinder with the outer surface (see Fig. 1) for the simulation's spherical shell radius ratio ($\chi = 0.9$). The same radius ratio was used to obtain predicted jets widths for Jupiter.

METHODS

Numerical modelling. The pseudo-spectral numerical code uses mixed implicit/explicit time stepping and has been benchmarked[28]. Values of non-dimensional control parameters[28] for the simulation are as follows: $\chi = 0.9$, $E = 3 \times 10^{-6}$, $\mathrm{Ra} = 1.67 \times 10^{10}$, $\mathrm{Pr} = 0.1$. Output parameters are measured to be approximately $\mathrm{Re} = 5 \times 10^4$ and $\mathrm{Ro} = 0.012$. The radius ratio $\chi = r_i/r_o$, where r_i and r_o are the inner and outer boundary radii, defines the spherical shell geometry. The Ekman number E is the ratio of viscous and Coriolis forces. The Rayleigh number Ra gives the strength of buoyancy forces in the flow. The Prandtl number Pr is the ratio of viscous and thermal diffusion. The Reynolds number Re is the ratio of inertial and viscous forces. The Rossby number Ro is the ratio of inertial and Coriolis forces. The top and bottom velocity boundary conditions are mechanically impenetrable and stress-free. The thermal boundary conditions are fixed temperature. The initial conditions are zero motion relative to the rotating frame and a random thermal perturbation, from which convection develops. Solving the governing equations on an 8-fold azimuthally truncated sphere[29], we use 768 points in latitude, 192 points in longitude and 65 points in radius. Convergence of the numerical simulation required the use of hyperdiffusion, which was reduced as the calculation became steadier in time. The hyperdiffusion has the same functional form (but with 1/10 of the final strength) of previous dynamo models[30]. The Ekman number was also lowered in stages. After E was reduced from 3×10^{-5} to 3×10^{-6} the model was run for over 1,600 planetary rotations and the convective motions approached a quasi-steady state. The total calculation time represents about 2,200 rotations and 0.14 viscous diffusion times.

Analysis of jet scaling. In meteorology and oceanography, the β-plane approximation is often used to represent flows in a very thin spherical shell by two-dimensional motions on a spherical surface. In this approximation, the Rhines length (which sets the latitudinal scale of zonal jets) is:

$$L_\beta = \left(\frac{V r_o}{\Omega \cos\theta}\right)^{1/2} \quad (1)$$

where θ is the latitude and V is a zonal flow velocity scale.

Convection in rapidly rotating deep spherical shells is largely invariant along the direction of the rotation axis, that is, in the z direction. The resulting flows are quasigeostrophic. In the limit of rapid rotation, flow becomes two-dimensional and is called geostrophic. The geostrophic Rhines length then refers to the scale in the cylindrical radius directions s:

$$L_g = \left(\frac{V}{\Omega}\frac{h}{|\partial h/\partial s|}\right)^{1/2} \quad (2)$$

The Rhines length now depends on the variation of the spherical shell height $h(s)$, measured in the direction of the rotation axis. This height dependence is referred to as the topographic β-effect[13]. Figure 2 demonstrates that the flow of our numerical simulation is indeed dominated by strong quasi-geostrophic zonal flows: the flow has a high degree of cylindrical symmetry and depends mainly on cylindrical radius.

The scales L_β and L_g are similar in many ways: both are based on two-dimensional approximations for a three-dimensional system[13]. However, a profound difference between the β-plane and geostrophic approximations is the existence of a tangent cylinder, which represents a discontinuity in the Rhines scaling. The height $h(s)$ doubles discontinuously outward across the tangent cylinder, while $\partial h/\partial s$ changes sign. Furthermore, stretching of fluid columns inhibits flow across the tangent cylinder. This effectively isolates the flow fields, suggesting that zonal flow scaling can be analysed separately inside and outside the tangent cylinder.

Accordingly, we take the Rhines length to be constant within each of the three regions bounded by the tangent cylinder (north, equatorial and south). Using this assumption we have derived a precise mapping from the observed regional velocity V to the predicted regional Rhines wavelength, given here in radians of latitude:

$$\lambda_g = 2\pi\left(\frac{V}{r_o \Omega C(\chi)}\right)^{1/2} \quad (3)$$

where $C(\chi)$ is a geometrical parameter containing latitudinal mean changes in the spherical shell height for the distinct regions inside and outside the tangent cylinder (see Supplementary Information for details). The regional Rhines widths $\lambda/2$ are compared with the measured jet widths of Jupiter and the numerical simulation in Fig. 3.

Received 18 May; accepted 1 September 2005.

1. Porco, C. C. *et al.* Cassini imaging of Jupiter's atmosphere, satellites and rings. *Science* **299,** 1541–1547 (2003).
2. Vasavada, A. R. & Showman, A. P. Jovian atmospheric dynamics: an update after Galileo and Cassini. *Rep. Prog. Phys.* **68,** 1935–1996 (2005).
3. Ingersoll, A. P. Pioneer 10 and 11 observations and the dynamics of Jupiter's atmosphere. *Icarus* **29,** 245–253 (1976).
4. Pirraglia, J. A. Meridional energy balance of Jupiter. *Icarus* **59,** 169–176 (1984).
5. Guillot, T., Stevenson, D. J., Hubbard, W. & Saumon, D. in *Jupiter, the Planet, Satellites and Magnetosphere* (eds Bagenal, F., Dowling, T. E. & McKinnon, W. B.) 35–57 (Cambridge Univ. Press, Cambridge, 2004).
6. Cho, J. Y.-K. & Polvani, L. M. The morphogenesis of bands and zonal winds in the atmospheres on the giant outer planets. *Science* **273,** 335–337 (1996).
7. Williams, G. P. Planetary circulations. 1. Barotropic representation of Jovian and terrestrial turbulence. *J. Atmos. Sci.* **35,** 1399–1426 (1978).
8. Williams, G. P. Jovian dynamics. Part III: Multiple, migrating, and equatorial jets. *J. Atmos. Sci.* **60,** 1270–1296 (2003).
9. Aurnou, J. M. & Olson, P. L. Strong zonal winds from thermal convection in a rotating spherical shell. *Geophys. Res. Lett.* **28,** 2557–2559 (2001).
10. Christensen, U. R. Zonal flow driven by deep convection on the major planets. *Geophys. Res. Lett.* **28,** 2553–2556 (2001).
11. Christensen, U. R. Zonal flow driven by strongly supercritical convection in rotating spherical shells. *J. Fluid Mech.* **470,** 115–133 (2002).
12. Yano, J. I., Talagrand, O. & Drossart, P. Origins of atmospheric zonal winds. *Nature* **421,** 36 (2003).
13. Yano, J. I., Talagrand, O. & Drossart, P. Deep two-dimensional turbulence: An idealized model for atmospheric jets of the giant outer planets. *Geophys. Astrophys. Fluid Dyn.* **99,** 137–150 (2005).
14. Aurnou, J. M. & Heimpel, M. H. Zonal jets in rotating convection with mixed mechanical boundary conditions. *Icarus* **169,** 492–498 (2004).
15. Ingersoll, A. P. Atmospheric dynamics of the outer planets. *Science* **248,** 308–315 (1990).
16. Rhines, P. B. Waves and turbulence on a beta-plane. *J. Fluid Mech.* **69,** 417–443 (1975).
17. Schoff, R. & Colin de Verdiere, A. Taylor columns between concentric spheres. *Geophys. Astrophys. Fluid Dyn.* **86,** 43–73 (1997).
18. Busse, F. H. A simple model of convection in the Jovian atmosphere. *Icarus* **20,** 255–260 (1976).
19. Manneville, J. B. & Olson, P. Banded convection in rotating fluid spheres and the circulation of the Jovian atmosphere. *Icarus* **122,** 242–250 (1996).
20. Jones, C. A., Rotvig, J. & Abdulrahman, A. Multiple jets and zonal flow on Jupiter. *Geophys. Res. Lett.* **30,** doi:10.1029/2003GL016980 (2003).
21. Read, P. L. *et al.* Jupiter's and Saturn's convectively driven banded jets in the laboratory. *Geophys. Res. Lett.* **31,** doi:10.1029/2004GL020106 (2004).
22. Atkinson, D. H., Pollack, J. B. & Seiff, A. The Galileo Probe Doppler Wind Experiment: Measurement of the deep zonal winds on Jupiter. *J. Geophys. Res.* **103,** 22911–22928 (1998).
23. Kirk, R. L. & Stevenson, D. J. Hydromagnetic constraints on deep zonal flow in the giant planets. *Astrophys. J.* **316,** 836–846 (1987).
24. Aubert, J., Brito, D., Nataf, H.-C., Cardin, P. & Masson, J. P. A systematic experimental study of spherical shell convection in water and liquid gallium. *Phys. Earth. Planet. Inter.* **128,** 51–74 (2001).
25. Evonuk, M. & Glatzmaier, G. A. 2D studies of various approximations used for modeling convection in the giant planets. *Geophys. Astrophys. Fluid Dyn.* **98,** 241–255 (2004).
26. Hubbard, W. B. Gravitational signature of Jupiter's deep zonal flows. *Icarus* **137,** 357–359 (1999).
27. Martinez, C. NASA selects new frontier mission concept study. ⟨http://www.jpl.nasa.gov/news/news.cfm?release=2005-090⟩ (2005).
28. Wicht, J. Inner-core conductivity in numerical dynamo simulations. *Phys. Earth Planet. Inter.* **132,** 281–302 (2002).
29. Al-Shamali, F. M., Heimpel, M. H. & Aurnou, J. M. Varying the spherical shell geometry in rotating thermal convection. *Geophys. Astrophys. Fluid Dyn.* **98,** 153–169 (2004).
30. Kuang, W.-J. & Bloxham, J. Numerical modeling of magnetohydrodynamic convection in a rapidly rotating spherical shell: Weak and strong field dynamo action. *J. Comp. Phys.* **153,** 51–81 (1999).

Supplementary Information is linked to the online version of the paper at www.nature.com/nature.

Acknowledgements Funding was provided by NSERC Canada, UCLA, and the DFG Germany priority programme 'Geomagnetic variations'. Computational resources were provided by the Western Canada Research Grid (West Grid).

Author Information Reprints and permissions information is available at npg.nature.com/reprintsandpermissions. The authors declare no competing financial interests. Correspondence and requests for materials should be addressed to M.H. (mheimpel@phys.ualberta.ca).